SNOW WATER EQUIVALENTS MODELED AT THE MESOSCALE WITH GEOGRAPHIC INFORMATION SYSTEMS

by

Jason Carey[1], and Rand Decker[2]

ABSTRACT[3]

Snow water equivalent (SWE) is spatially distributed within the mountainous basins of climates marked by a seasonal snowpack. This distribution is directly linked to mesoscale physiography such as slope, solar aspect, elevation, canopy, wind transport zones and avalanche tracks, and to time. In the Oquirrh Mountains near Salt Lake City, the SWE distribution of seven subbasins has been modeled with GIS technology and a DEM of the area. The purpose of the model is to obtain accurate estimates of SWE for smaller basins. The modeled subbasins are on the order of 1km^2.

Individual maps of mesoscale physiography were developed as the controls of SWE distribution. Daily, water year 1997 data from three SnoTel stations was compared with physiographic maps. Using snow accumulation theory and a statistical analysis of ground measured data, individual SWE distribution models were fit with the mesoscale models of solar aspect, elevation, vegetation and basin area. The SWE distribution models, representing either loss or gain, were then combined in chronological order to model total snow accumulation for a season.

Peak SWE was calculated for March 7, 1997 using the mesoscale accumulation model. A total SWE of 1882.74 acre-feet, 35.6% of average Bingham Canyon annual precipitation, was calculated for peak. Modeled site locations had a very good linear correlation (0.97) with measured site data. A ridge line cornice model contributed 51.99 acre-feet SWE, 2.7% of peak. The Snow Estimation and Updating System (SEUS) is implemented by the Colorado Basin River Forecast Center for macroscale SWE calculations. SEUS modeled 3569.35 acre-feet, 190% of the mesoscale model, for the same area and period. This study shows that the scale of the study area determines the influence of the mesoscale distribution on basin wide SWE determination.

INTRODUCTION

This is a study of modeling snow water equivalents (SWE). The goal is to accurately determine the amount of water in a spatially distributed snow pack for a small basin. This study area is located upgradient from the Kennecott Copper Pit in the upper basins of the eastern slope of the Oquirrh Mountains near Salt Lake City. As a result of mine workings the study area is on the order of 10km^2 over 7 escarped drainages. As a result of mine proximity an accurate model of SWE distribution is required.

Spatially distributed snow packs vary continuously; therefore, exact measurements of SWE are infinitely complex. Analogously, 'no two snowflakes are identical'. Because of the snow distribution complexity, SWE must be measured within scaled parameters. Distribution patterns of snow occur on all scales. The areal variability of snow cover is commonly considered on three geometric scales. McKay and Gray (1981) defined these as the macroscale, mesoscale and the microscale.

> Macroscale or regional scale: areas up to 10^6 km with characteristic linear distances of 10^4 to 10^5 m depending on latitude, elevation and orography, in which the dynamic meteorological effects such as standing waves, the directional flow of wind around barriers and lake effects are important. (p. 153)

---

[1]Master of Science, Civil Engineering, University of Utah, Salt Lake City, Utah 84112

[2]Professor of Civil Engineering, University of Utah, Salt Lake City, Utah 84112

[3]Presented at the Western Snow Conference, 1998

Snow hydrology is usually involved at the macroscale, determining SWE for large watersheds. Here the areal extent of snow cover may dominate SWE calculations and the variables of density or depth of snow at a point may be insignificant. At the other end of the spectrum, the microscale, SWE accumulation can vary within short distances.

- Microscale: Characteristic distances of 10m to 100m over which major differences occur and the accumulation patterns result from numerous interactions, but primarily between surface roughness and transport phenomena.

For instance, one side of a tree may have much more snow than the other. Stratigraphy, and density changes, local ablation changes, and effects of long wave radiation can all affect the SWE accumulation at the microscale. Point measurements, such as snow pillows and snow courses, are all measures of the microscale. A collection of point sources is often extrapolated into the macroscale and all microscale anomalies are considered insignificant or expected to average over the larger scale. Under the lens of the mesoscale, the microscale anomalies can be averaged within the mesorelief zones that have a significant effect on snow accumulation.

- Mesoscale or local (within region) scale: characteristic linear distances of 100m to 1000m in which redistribution along mesorelief features may occur because of wind or avalanches and deposition and accumulation may be related to the elevation, slope and aspect of the terrain and to the canopy and crop density, tree species or crop type, height, extent and completeness of vegetative cover.

Consider a forest. At the microscale many accumulation patterns can be recognized: tree wells, drifts in clearings, interception in branches. However, these patterns may not vary significantly throughout the forest when compared on the local scale to a unforested slope that absorbs high amounts of solar radiation and experiences midseason melts.

In mountainous terrain the seasonal snow cover distribution is highly dependent on the mesorelief features. These features affect distribution of both the initial precipitation and the temporal redistribution of snow. A complex areal accumulation of snow cover results. The dynamics of snow accumulation are directly dependent on physical parameters, including atmospheric and surface variables. These parameters are infinitely complex in the fact that they vary continuously spatially and temporally. Analogously, no two mountains are identical or no two storm events are identical. This makes it not only difficult to model distribution precisely but also infinitely complex to model the snow distribution variables. However, the temporal and spatial consistency of the mesorelief physiography results in a statistical consistency for SWE distribution at the mesoscale. Defined mesorelief physiography will determine SWE distribution patterns at the mesoscale.

STUDY AREA

Upgradient from the mine workings of Kennecott Copper Pit, 7 escarped basins collect a seasonal and highly distributed snowpack. Aspects of the basins are generally leeward, with winds prevailing 63 to 39% from the west, and 18 to 21% from the south. Annual precipitation in the Oquirrh ranges from 20in to 40in, with 25in averaging in Bingham canyon, the principal drainage of this study. Spring and summer evaporation rates exceed precipitation. Elevations range between 6400ft and 9207ft at Clipper Peak. The latitudes of the study are within 40°30' to 40°35' North.

Access to the study area was restricted by KUC policy. However visual observations were made on April 26, 1997:11:00 mst from the visitor center parking lot at 6800ft. Although limited in their scope, these observations revealed many mesoscale distribution patterns. Cornices lined all major ridges, and sluffing zones were evident below the cornices. Vegetation was mainly ground shrub, with sparse deciduous stands on the northern aspects of the larger peaks and coniferous stands were only evident on the north face of West Mountain and Galena Gulch. The contrast of solar aspect was highly evident (Fig. 1). Southern tending slopes throughout the study area were barren of snow to the cornice line. These slopes revealed the shrub ground cover while the northern slopes were blanketed in snow. The study area represents mid latitudes at mid altitudes and typically experiences mid season melts. Furthermore, the study area has a simplified mesoscale physiography; no avalanche activity has been recorded, there is very little area of forest canopy and no perineal streams exist at the study area. Kennecott Utah Copper (KUC) provided 1997 water year data from two

FIG. 1. A section of the study area photographed on April 26, 1997.

SnoTel stations, and a digital elevation model (DEM) (Fig. 2) of the area resolved to 10ft x 10ft grids. Three basins of the eastern slope of the Oquirrh Mountains have installed SnoTel stations that record daily SWE change, precipitation accumulation and max/min temperature. Both the Sap (7420ft) and

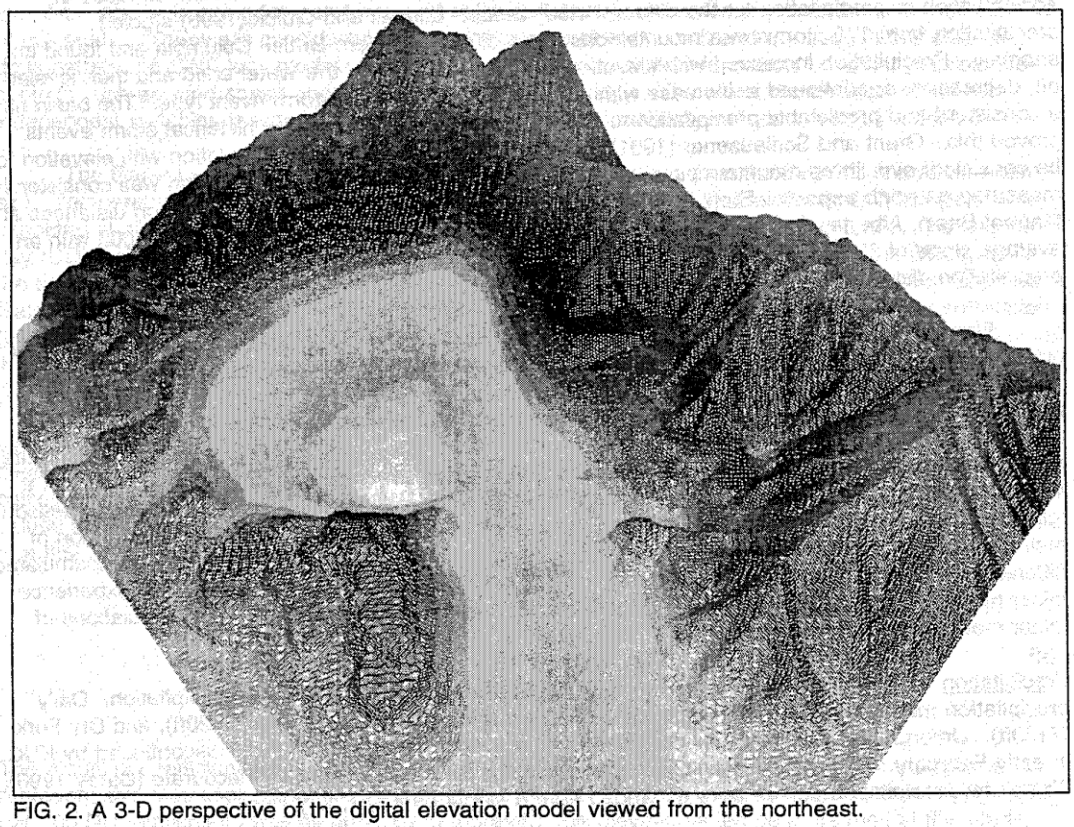

FIG. 2. A 3-D perspective of the digital elevation model viewed from the northeast.

Galena (7972ft) gauges are maintained by KUC and were installed in the fall of 1996. The Dry Fork SnoTel station is maintained by the Natural Resources Conservation Service (NRCS) and was installed in the fall of 1994. Dry Fork is the proximal basin to the north of the study area. This basin drains approximately 3.5mi.^{2} into Bingham Canyon.

MESOSCALE SWE DISTRIBUTION MODEL DEVELOPMENT

Development of the SWE distribution model was in seven steps. First, the mesoscale physiographic themes that control SWE accumulation were theorized. Second, models of the controlling physiography were developed from the DEM. Third, the controlling physiographic values were isolated and evaluated at each SnoTel site. Fourth, SWE distribution dependence upon each individual physiographic mesoscale feature was developed from statistical analyses of the measured SWE, precipitation, and temperature data. Fifth, SWE models were created by extrapolating the statistical results throughout each physiographic models. Sixth, the individual SWE models were summed for each period. Seventh, the period SWE models were summed in chronological order to represent the seasonal SWE evolution at the study site.

Elevational Snow Distribution

Snow cover distribution with elevation has been recognized by many studies. Elevational changes usually result in higher precipitation at higher elevations. A study conducted by the U.S. Army (1956) derived a linear relationship between snow accumulation and elevation; however, the ratio of snow to elevation was determined to be basin dependent. This relationship was also shown to have a temporal dependence, altering the ratio over the season but remaining linear with respect to elevation. Mieman (1970) has collected data from 11 independent studies in differing physiographic areas and all show a snow increase with elevation. However, these results show different elevational ratios of accumulation or precipitation for the different study areas. Loukas and Quick (1996) studied precipitation from 175 storms in a mountainous basin of southwestern British Columbia and found an anomaly. Precipitation increased with elevation up to middistance of the water shed and then leveled off, decreased, or continued to increase with elevation, depending on storm event type. The basin has a consistent and predictable precipitation to elevation relationship. Modeling historical storm events proved this. Grant and Schleusener (1961) found a direct correlation of accumulation with elevation to be consistent over three mountain passes in central Colorado. Deepest accumulation was consistently measured on north aspects. Storr (1967) found a wide precipitation variation within short distances at Marmot Basin, Alberta. The basin is 3.5 square miles in size and rises from 5200ft to 9200ft with an average slope of 39°. Storr concludes that the more rugged the terrain, the greater will be the precipitation distribution.

Physically the effects of elevation on SWE accumulation are partially explained by temperature gradients that vary, often directly, with altitude. Orographic lifting of storms can bring vapor through temperature gradients adiabatically, without a heat exchange. Saturated air is a function of temperature and warmer air can hold higher moisture contents before saturation. For instance, if the moisture content saturates air at one temperature, the air will not be saturated at a higher temperature. Similarly, lower air temperatures will remain saturated, but the excess moisture will precipitate. As a saturated air mass moves through decreasing temperatures, precipitation occurs. Through the season temperature gradients can further distribute a snow pack by melting. The seasonal accumulation of melt losses may change a snow pack's elevational distribution significantly because of the accumulated differences in above freezing temperature exposure. For example, lower elevations may experience minor melts daily, whereas upper elevations remain in subfreezing temperatures. Accumulations of minor melts may add up to a significant disparity.

Precipitation This study models the distribution of elevationally displaced precipitation. Daily precipitation measurements were made at all three sites, Galena (7972ft), Sap (7420ft), and Dry Fork (7160ft). Unfortunately, the Sap site precipitation gauge was malfunctioning and discontinued by KUC in early February. Furthermore, the Galena precipitation data are considered inaccurate (Carey 1998). Therefore, precipitation curves were expanded from a single data site, Dry Fork.

An arbitrary power scale curve was chosen to represent the study area

$$P = P_0 1.5^{\left(\frac{topo7200 - E_0}{1000}\right)} \quad (1)$$

where P_o(in) is the measured precipitation, *topo7200* (ft) is the DEM, E_o(ft) is the elevation of the measurement, and P(in) is the precipitation at an elevation. The relevancy of the applied precipitation curve was then checked with the positive SWE accumulation at the Galena and Sap sites. The precipitation gauges are designed with wind shields to prevent measurements of redistributed snow; however, accumulated SWE at the pillow measures precipitation as well as possible redistributed snow. The redistribution of snow can be extremely complicated and variable, often due to wind patterns and terrain features. Furthermore, precipitation may not record at the SWE gauge simultaneously with the precipitation gauge. In order to check the relevancy of the implemented power curve, 30-day accumulations of measured SWE were compared to 30-day accumulations of modeled precipitation at the sites. A good data correlation resulted for the applied curve. (Carey 1998) The applied precipitation curve is arbitrary, and the lack of data renders this calculation inconclusive. However, the good comparison of SWE deposition to precipitation modeled at the sites does show that the precipitation curve is within the scale of the study and therefore applicable within the errors of the data.

Temperature Loss The peak SWE at Sap Gulch measured only 61.2% of the peak measured at Galena. Intuitively, an elevation difference of 552ft is not significant in describing this disparity due singularly to elevational precipitation gain. Redeposition and SWE loss factors must be considered to explain this disparity. The measured loss at a site can be due to a number of physical processes including solar energy, heat, and wind scouring. Determination of controlling SWE loss variables is site specific. Above freezing temperatures and solar radiation were implemented as the sole melt controls of this study. These are considered major constituents of snow melt and are used in this study to demonstrate the SWE loss model. Recorded data did not include information for other possible loss controls such as wind speed and direction or relative humidity. Therefore, the analysis of the two independent variables results in other loss controls being statistically included in those modeled.

The Galena Gulch measurement site averaged 2.2°F cooler than the Sap Gulch measurement site. Temperature gradients are considered a function of elevation. The minimum daily temperatures, expected at night, show similar trends (2.3°F) and reinforce the elevational dependence. The degree day (DD) factor is examined to relate SWE loss with above freezing temperatures. The DD factor is the sum of a daily temperatures above freezing for a given period. DD differences between Sap and Galena data sites were calculated based on KUC average temperature data. A high linear correlation (0.98) between Sap and Galena DD site data was achieved. An average loss of 1.53 DD per day per 1000ft was statistically determined to be the representative elevational DD profile (Carey 1998).

In order to derive the contributions of the independent loss factors from the dependent SWE loss variable, an analysis was performed on the loss controls. For each time period the sum of the measured SWE daily losses, the accumulated solar irradiation, and the accumulated DD factor were calculated. A matrix was created (Equ. 2) to compare the measured dependent SWE loss values with values of the independent SWE loss factors according to accumulation period. The analysis was limited to a first-order equation with no constants.

$$\begin{array}{c|cccc|l} x & solar1 & solar2 & solar3 & solar4 & \ldots & \\ y & DD1 & DD2 & DD3 & DD4 & \ldots & z=ax+by \\ z & SWE1 & SWE2 & SWE3 & SWE4 & \ldots & \end{array} \quad (2)$$

The resulting coefficients of the independent variables were then considered to be the study area representative loss coefficients (Carey 1998). In conclusion of this analysis a loss factor of 0.7in SWE per 100 DD relationship was determined to represent the elevational temperature melt at this study.

Equation 3 models SWE loss, in hundredths of an inch, based on a linear DD elevational gradient where *ddloss(date)* (Fig. 3) maps the SWE loss,

$$ddloss(date) = 0.7\left(\frac{topo7200 - E_0}{1000} \times 1.53 \times T - D_0\right)(IFF \leq 0) \quad (3)$$

topo7200 is the DEM, (D_o) the accumulated DD measured at a site, the measurement site elevation is (E_o), the DD loss per 1000ft per day factor is (1.53in), (T) is the number of days in an accumulation period, and the SWE loss per DD factor is (.007in). A conditional modeling algorithm (IFF<=0) was included to represent the elevational freezing point where no losses due to DD occurred at or above. Model ddloss37 (Fig. 3) shows the DD gradient and the freezing line for the accumulation period February 28, to March 7, 1997, the Galena site is above this line. A cumulative, elevationally dependent, DD controlled, SWE loss model resulted.

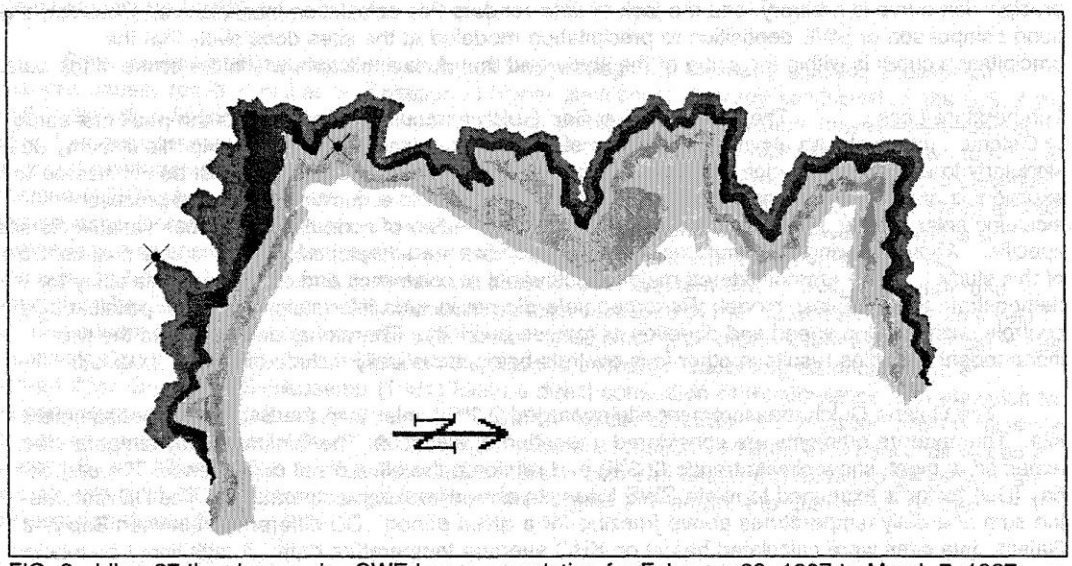

FIG. 3. ddloss37 the degree day SWE loss accumulation for February 28, 1997 to March 7, 1997. The KUC measurement sites are marked and the Galena site is above the freezing line.

Solar Aspect Snow Distribution

The effect of solar aspect is typically one of melt and loss (Meiman 1971). Solar aspect is the incident angle of a solar ray on the surface of the earth. The solar aspect is a function of the slope and aspect of the surface, and the declination and azimuth of the sun. The potential solar energy at the surface is a function of the exposure time which is also solar aspect dependent. Unshaded southern aspects (in the Northern Hemisphere) can expect exposure times equal to the full day at latitude. In comparison a vertical wall with an eastern or western aspect would be exposed for only half of the day. The accumulation of solar energy is highly varied in mountainous areas.

Short wave radiation is emitted by the sun at wavelengths of .2 to 2.2μm. At the outer atmosphere, incident radiation flux is 1.365kw/m^2 +- 7% due to earth's varying orbit. Atmospheric conditions determine the amount of direct short wave radiation that reaches the surface of earth. Clouds scatter while dust, CO_2, Ozone, and water vapor absorb shortwave radiation and emit long wave radiation, measured as heat. The declination of the sun determines the path, and, therefore the

amount of atmosphere that scatters and absorbs shortwave radiation. The maximum path length occurs during the winter solstice. As the sun's declination decreases towards summer, incident radiation at a surface increases and exposure times increase. At 40° latitude, the minimum solar declination is 16.7°, and the maximum exposure time is 14.86 hours (Frank et al, 1966).

Surface features can have a major effect on short wave radiation. The albedo index is defined

$$A = \frac{Q_r}{Q_{is}} \quad (4)$$

as the ratio of reflected shortwave radiation (Q_r) to the incident short wave radiation (Q_{is}) at a surface. Greater radiation reflection results in a higher the albedo index. The albedo of a snow pack is effected by many variables. Short wave reflection by snow is highly controlled by surface properties such as grain type and size (Male and Gray, 1981). Light dry snow usually has a very high albedo, 90% reflection can be expected. Albedo can also be affected by purity and transparency. Shallow snow packs can be transparent for short wave radiation reaching the ground level. This causes a higher absorption and lower albedo. Dirty snow pack affects albedo similarly. A snowpack's albedo index can change over a season. Decreasing albedo with increasing snow density has been reported by Male et al. (1981). Surface properties affect the albedo of a snowpack at a point for a given incident radiation and vary at the microscale.

At the mesoscale, more predictably and to a greater seasonal accumulation effect, solar aspects control albedo indices. Incident solar radiation is dependent on the solar aspect of the surface. Albedo indices decrease as incident angles of solar radiation increase. Mathematically, this is due to the increasing denominator of the albedo index (Equ. 4). At a surface, incident angles are determined by solar declination as well as local slope and solar aspect. The culmination of these effects is often seen when south faces (in the Northern Hemisphere) melt earlier in the season and often have a lower SWE totals due to midseason snow melt losses.

A solar aspect theme was developed with the combination of a slope theme in 10% increments, and an aspect theme for 16 azimuths. Solar irradiation accumulation models *r(date)* were created from tables (Frank et al.) applied to the solar aspect theme. The solar irradiation models represent maximum potential irradiation.

Cumulated loss models were run for the consecutive SWE accumulation periods. Models of SWE loss due to solar radiation were created based on the solar irradiation accumulation and the loss coefficient obtained in the numerical loss analysis of equation 3. Models *solarmelt(date)* (Equ. 5):

$$solarmelt(date) = r(date) \times 0.27 \quad (5)$$

were created using the relationship of 0.27 inches SWE loss per kilo-Langley (kg-cal/cm^2) exposure (Carey 1998) and continuously integrating over the entire study area. Maps *solarmelt(date)* (Fig. 4) model SWE loss in hundredths of an inch as a function of solar irradiation.

Wind Transport

Wind redistribution of snow is a major feature in mountain snow packs. Wind flow patterns that scour and deposit snow are scaled with mesorelief features. Windward slopes typically cause an acceleration of wind speeds. On the lee of a crest there is a large pressure drop and a deceleration of wind speeds. With slowing wind speeds, flows can separate, become turbulent, eddy, and deposit snow. The transport phenomenon is more complicated than addressed herein; however, light dry snow can transport with wind speeds near 5m/s (McClung and Schaerer,1993) and deposit at lesser speeds.

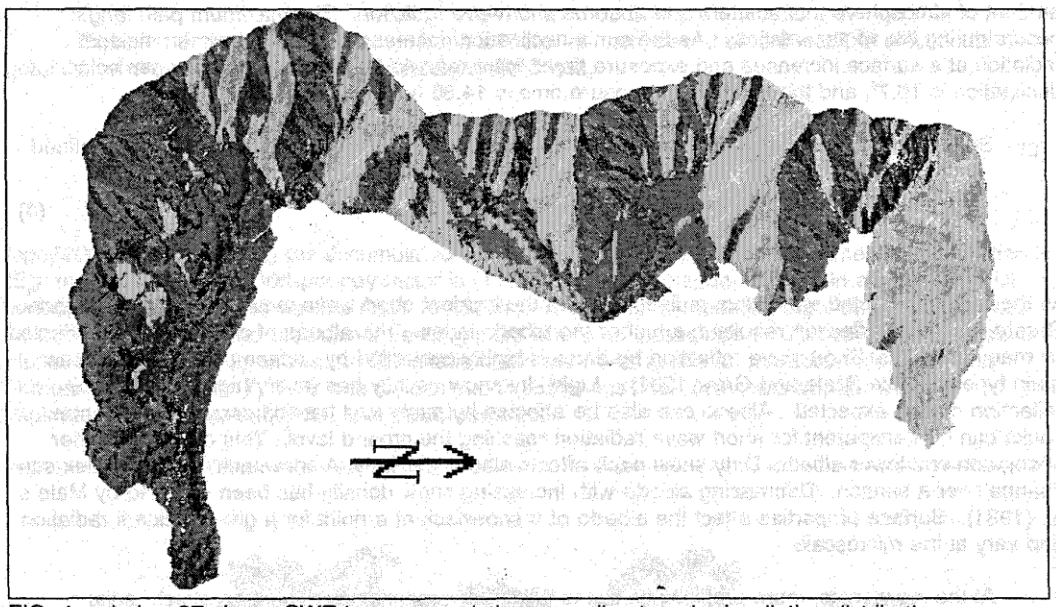

FIG. 4. solarloss37 shows SWE loss accumulation according to solar irradiation distribution accumulated as of March 7, 1997. The measurement sites are marked.

Wind can move a significant amount of snow from one basin to another. Cornices built on leeward edges of mountainous ridge lines are an omnipresent example of wind transport. Large drifts can similarly build in lee basins. McClung and Schaerer (1993) found that lee zones can collect three to five times, and higher, the amount of snow in nearby wind protected areas. This interbasin transport can deposit or scour SWE not accounted for by precipitation measurements. Montange (et al., 1966) estimated 54 acre-feet SWE existed in the cornices of their study; 1% of the total SWE in the Maynard Creek watershed. The observed cornices in Maynard Creek measured 10m in height by 15m in leeward fetch length. The studied crest line was 2.5km in length. Using an estimated value for the average cornice density of 300kg/m^3, Montange calculated cornice SWE by the feature geometry.

Cornice features were evident in visual observations (Fig. 1). SWE distribution models were developed in order to determine the contribution of cornice features to total SWE calculations. The cornice model implemented in this study is empirical. A geometric wedge was used to represent a cornice. The lack of data required the assignment of objective values for the cornice wedge dimensions.

Cornices typically build on the lee of major ridge lines. The map *corniceridge* represents the empirical lee ridge line. The *cornice* model is the length dimension of *corniceridge* with a width dimension that represented a cornice fetch length. The fetch is the lee dimension of the cornice. Fetch lengths of 30ft were used to demonstrate the model and approximate cornice dimensions. Considering the cornice as a wedge, the ridge areas were then expanded in volume. For modeling purposes, a cornice face dimension of 15 feet was used. The cornice density factor of 0.35 was multiplied to achieve a SWE. For *cornice* (Equ. 6):

$$cornice = corniceridge \times 0.5 f \times d \times \frac{\rho}{\rho_w} \qquad (6)$$

f is the fetch length (ft) , d the depth (ft), ρ the density of the cornice feature, and ρ_w the density of water. For the principal lee ridge, the cornice model contributed 52 acre-feet SWE. This added SWE is not accounted for in precipitation gains; cornice SWE represents an interbasin mass change.

Model of Seasonal Accumulation

A model of seasonal SWE accumulation was created to show the cumulative effect of the individual and the incremental SWE distribution models. Individual SWE distribution models, elevational precipitation, DD loss, solar loss, and cornice accumulation were created for each period of the snow season and then summed to represent an incremental distribution. Cornice distribution was summed with the maximum accumulation period only. The incremental distributions were then summed according to chronological order (Equ. 7):

$$accum(date) = accum(prev) + precip15(date) + ddloss(date) + solarmelt(date) + cornice(IFF \geq 0) \quad (7)$$

where an algorithm to disregard excess loss values (IFF>=0) was included. For each seasonal accumulation period modeled, total SWE volume and the located site SWE (Galena and Sap) were calculated. Table 1 shows these values in acre-feet for total volume and hundredths of an inch SWE for the sites. The Sap site modeled to measured data had a correlation of 0.97 and the Galena modeled to measured data had a correlation of 0.89. Peak variances were small for both modeled sites. The peak total SWE for the entire study area was modeled as 1882.74 acre-feet Fig. 5). Over the total modeled basin area of 2552.54 acres, the peak snow pack would average of 8.9in SWE, 35.6% of the average Bingham Canyon yearly precipitation.

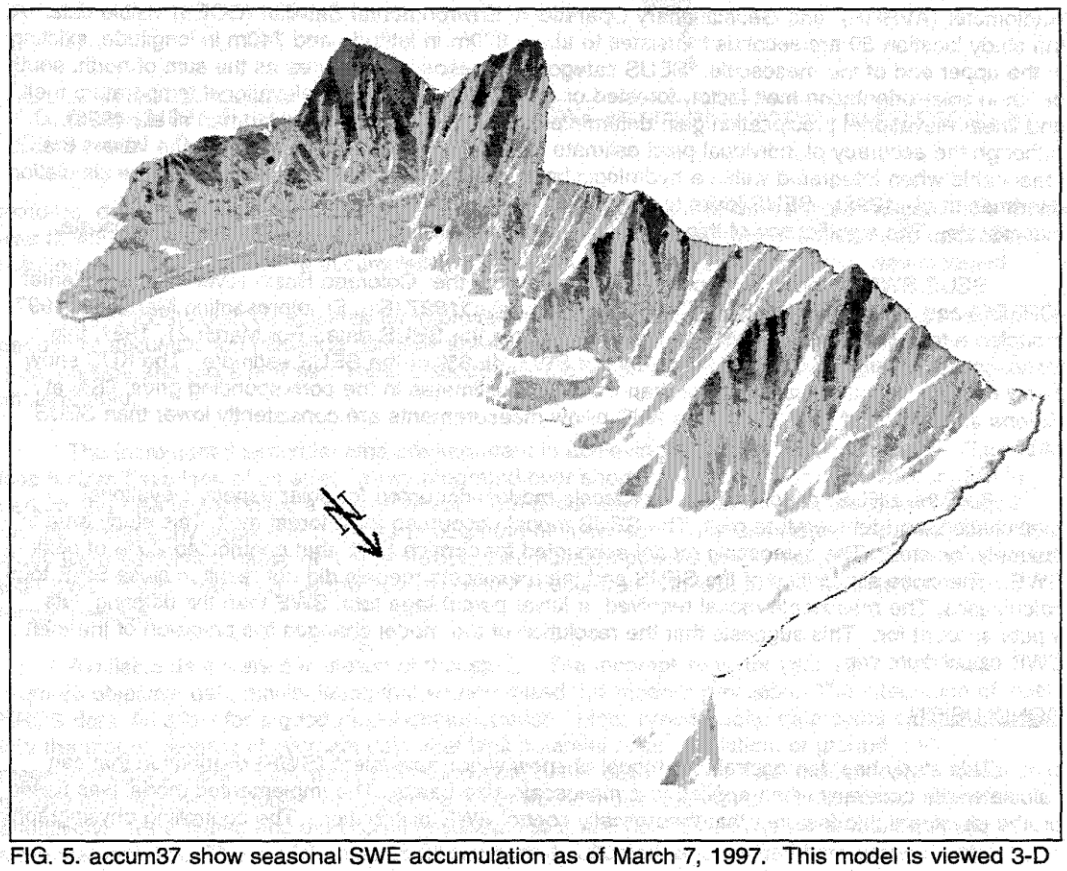

FIG. 5. accum37 show seasonal SWE accumulation as of March 7, 1997. This model is viewed 3-D over the northeast shoulder of Freeman Peak.

Table 1

	Sap Modeled SWE 100*in	Galena Modeled SWE 100*in	Sap Measured SWE 100*in	Galena Measured SWE 100*in	Volume Modeled acre-feet
Nov 30	302	612	93	559	604.56
Jan 31	944	1576	621	1176	1799.68
March 7	1030	1827	1002	1773	1882.74
March 21	839	1665	701	1636	1665.05
April 4	573	1458	464	1605	1433.25
April 19	335	1261	51	1436	1254.92
May 3	280	1342	8	1223	1344.04
cornice					51.99
seus31897 (macroscale model)					3569.35

MACROSCALE COMPARISON

The National Operational Hydrologic Remote Sensing Center (NOHRSC) maintains a database of snow coverage for the western United States. The Snow Estimation and Updating System (SEUS) is implemented by NOHRSC for the Colorado River Basin, parts of the Sierra Nevada and Oregon. SEUS takes input from imaging satellites, gamma flight lines, SnoTel, and snow course measurements and models the information with a DEM to create areal SWE estimations. SEUS maps provided by NOHRSC are resolved to 30 arc seconds, the resolution of the Advanced Very High Resolution Radiometer (AVHRR) and Geostationary Operational Environmental Satellite (GOES) visible data. At the study location 30 arc seconds translates to about 870m in latitude and 740m in longitude, existing in the upper end of the mesoscale. SEUS categorizes mesoscale features as the sum of north, south or flat in solar orientation melt factor, forested or unforested melt factor, elevational temperature melt, and linear elevational precipitation gain determined from the no-snow line (Hartman et al., 1996). Although the accuracy of individual pixel estimate from SEUS may be questionable, the values are reasonable when integrated within a hydrologic basin and provide for improved stream flow simulation (Hartman et al., 1995). SEUS looks to mesoscale features in order to gain accuracy at the macroscale. The significance of this study is to find SWE distribution accuracy at the mesoscale.

SEUS SWE distribution maps were obtained from the Colorado Basin River Forecast Center (CRBFC) and overlaid on the KUC DEM. The map *seus31897* (Fig. 5), representing March 18, 1997, modeled a total SWE of 3569.35 acre-feet directly from the SEUS data. For March 21, 1997, this mesoscale study modeled 1665.05 acre-feet of SWE, 46.6% of the SEUS estimate. The KUC snow pillow data for March averaged lower than the SEUS estimates in the corresponding grids: 88% at Galena and 60.1% at Sap Gulch. The KUC pillow measurements are consistently lower than SEUS data.

Both the SEUS model and the mesoscale model accounted for solar aspect, elevational precipitation, and temperature melt. The SEUS model accounted for a forest melt. This study area is sparsely forested. The mesoscale model accounted for cornice SWE that contributed 2.7% of peak SWE. The close similarities of the SEUS and the mesoscale models did not result in close SWE total calculations. The mesoscale model resolved a lower percentage total SWE than the differing data inputs account for. This suggests that the resolution of the model changes the precision of the total SWE calculation.

CONCLUSION

This study has demonstrated a model of snow water equivalent (SWE) distribution that can calculate with accuracy when applied to a mesoscale size basin. The implemented model was based on the physiographic features that theoretically control SWE distribution. The controlling physiographic

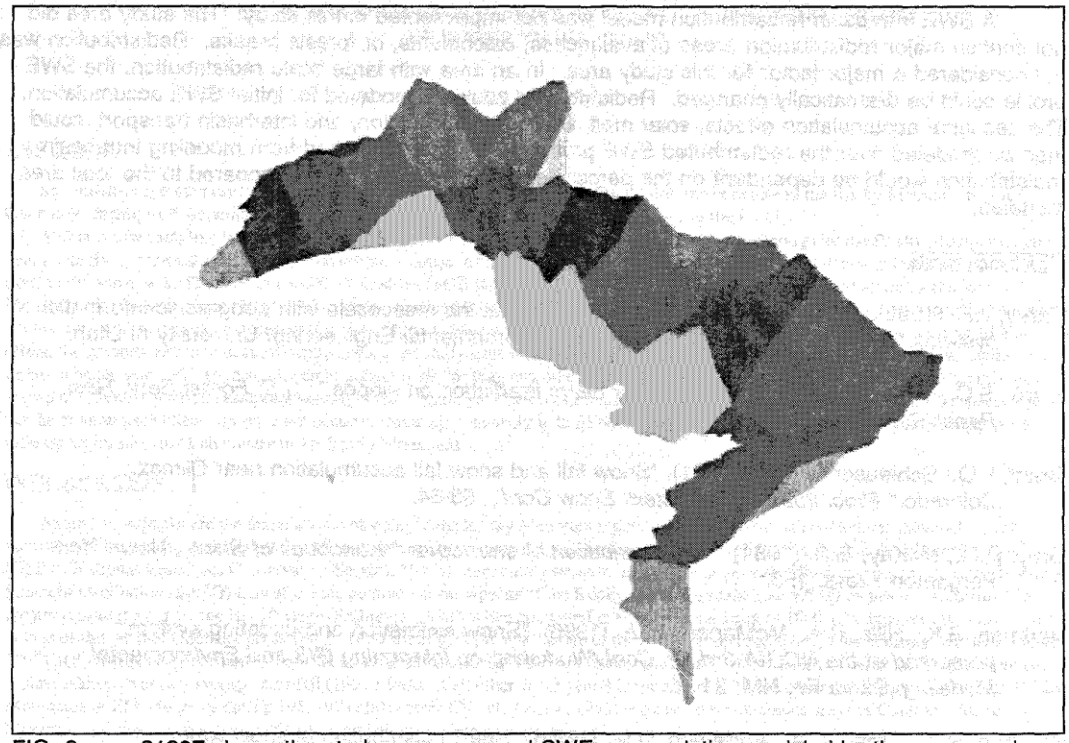

FIG. 6. seus31897 shows the study area seasonal SWE accumulation modeled by the macroscale SEUS model. The view is 3-D from the northeast.

features demonstrated in this model were elevation, solar aspect and wind-affected ridges. The model was fit with measured site data. A good correlation between the modeled and measured data sites resulted, and reasonable peak accumulation, 35.6% of yearly average precipitation, was modeled.

This model could be adjusted for improvement in three distinct ways. First, the incremental periods of accumulation modeling could be shortened. Second, data measurements could be both more diverse and more precise. Third, a secondary model of intrabasin redistribution could be implemented.

The incremental period lengths are important in achieving accuracy from this model. Excess loss factors have less of an effect when integrated over shorter periods. Over longer accumulation periods the loss factors have a greater effect. The accumulation periods of this study were long, 2 months in the early season to 2 weeks through the melt season. The loss factors implemented in this study were calculated based on the two-week accumulation periods of the melt season. The modeled total SWE of this study may be low due to greater effects from the loss factors modeled over the longer periods.

Available data were a limitation of this study. The incomplete water year 1997 KUC data, required objective data manipulation that compromised the model's precision. The integration of local NRCS data did allow for a good model demonstration. More precise solar data could be implemented into the model; records of overcast days that limit potential solar irradiation, or ground truth measurements of direct short wave radiation would better calibrate the solar melt models. Measured density and dimension values of cornice features would model the interbasin distribution more effectively. Wind speed and direction measurements would help determine redistribution trends at a measurement site. The model could be further tested, adjusted, and verified from ground truths.

A SWE intrabasin redistribution model was not implemented in this study. The study area did not contain major redistribution areas of avalanches, catchments, or forests breaks. Redistribution was not considered a major factor for this study area. In an area with large scale redistribution, the SWE profile could be dramatically changed. Redistribution could be modeled for initial SWE accumulation. The seasonal accumulation effects, solar melt, DD loss, precipitation, and interbasin transport, could then be modeled over the redistributed SWE profile. The accuracy gained from modeling intrabasin redistribution would be dependent on the percentage of redistribution area compared to the total area modeled.

REFERENCES

Carey, J.P. (1998). "Modeling snow water equivalents at the mesoscale with geographic information systems." Thesis (M.S.), Dept. of Civil and Environmental Engineering, University of Utah.

Frank, E.C., Lee, R. (1966). "Potential solar beam irradiation on slopes." *U.S. Forest Serv. Resr. Paper RM-18.* Fort Collins, CO.

Grant, L.O., Schleusener, R.A. (1961). "Snow fall and snow fall accumulation near Climax, Colorado." *Proc. 29th Ann. Western Snow Conf.*, 53-64.

Gray, D.M., McKay, G.A. (1981). "The distribution of snowcover." *Handbook of Snow* , New York, Pergamon Press, 153.

Hartman, R.K. ,Hills, R.A., McManamon, A. (1996). "Snow estimation and updating system," *presented at the NCGIA 3rd Int. Conf./Workshop on Integrating GIS and Environmental Modeling* ,Santa Fe, NM, 21-25.

Hartman, R. K., Rost, A. A., Anderson, D.M. (1995). "Spatial distribution of snow water equivalent observations in mountainous terrain." http://www.nohrsc.nws.gov/html/papers/spatial/spatial.htm.

Loukas, A., Quick, M.C. (1996). "Spatial and temporal distribution of storm precipitation in southwestern Brittish Columbia." *J. Hydrology*, 174, 37-56.

Male, D.H., Gray, D.M. (1981). "Snowcover ablation and runoff." *Handbook of Snow*, New York , Pergamon Press, 360.

McClung, D., Schaerer,P. (1993). *The Avalanche Handbook*, Douglas & McIntyre, Ltd., Vancouver, B.C..

Meiman, J.R. (1970). "Snow accumulation related to elevation, aspect and forest canopy." *Snow Hydrology: Canada Nat. Comm. for the Int. Hydrologic Decade.*

Meiman, J.R., Remmenga, E., Keller, H. (1979). "Snow distribution in relation to solar irradiation on two Swiss pre-Alp watersheds." *Water Resour. Resr.*, 7(6), 1636-1640.

Montange, J.R., McPartland, J.T., Super, A.B., Townes, H.W. (1968). "The nature and control of snow cornices on the Bridger Range southwest Montana." *Alta Avalanche Study Center, misc. Report #14,* Montana St. Univ., Bozeman, MT.

Storr, D. (1967). "Precipitation variations in a small forested watershed." *Proc. 35th Ann. Western Snow Conf.,* 11-17.

United States Army Corps of Engineers (1956). *Snow hydrology; summary report of the snow investigations.* Portland, Or., North Pacific Division Corps of Engineers, U.S. Army.